ISSN 1063-7834, Physics of the Solid State, 2013, Vol. 55, No. 12, pp. 2596–2601. © Pleiades Publishing, Ltd., 2013.
Original Russian Text © A.N. Korol', V.N. Isai, 2013, published in Fizika Tverdogo Tela, 2013, Vol. 55, No. 12, pp. 2468–2473.

GRAPHENES

Energy Spectrum of the Fibonacci Graphene Superlattice

A. N. Korol'[a, b, *] and V. N. Isai[a]

[a] *National University of Food Technologies, ul. Volodymyrska 68, Kyiv, 01601 Ukraine*

[b] *Laboratory on Quantum Theory in Linköping, International Society for Independent Research (ISIR), Box 8017, Linköping, 580 80 Sweden*

* *e-mail: korolam@ukr.net*

Received March 11, 2013; in final form, May 30, 2013

Abstract— Energy spectra of the graphene-based Fibonacci superlattice (SL) in the presence of the forbidden band in graphene have been investigated. The lattice consists of rectangular barriers, which are arranged along axis *Ox*. The quasi-periodic modulation is performed due to the difference in the values of the mass summand of the Hamiltonian in various SL elements. It is shown that effective splitting of allowed bands (and thereby the formation of a series of gaps) under the effect of the quasi-periodic factor is implemented with both inclined and normal incidence of the electron wave on the SL surface. The energy spectra have the clearly pronounced periodic character over the entire energy scale. The bands split in separate fragments of the spectrum (conventionally periods) according to the Fibonacci inflation rule in each new generation. The forbidden band associated with a new Dirac point is formed in all Fibonacci generations similarly to the periodic graphene-based SLs. The location of the Dirac point is independent of the SL period; it is very sensitive to the potential barrier height and to the width ratio between the quantum well and the barrier, and depends weakly on the mass summand in the Hamiltonian. The dependence of the spectra on the incidence angle of the electron wave is insignificant.

DOI: 10.1134/S1063783413120147

1. INTRODUCTION

It is known that semiconductor superlattices (SLs) can play an essential role in controlling the electron processes in various devices of modern electronics (see, e.g., [1]). Therefore, great attention is paid to the investigation of physical properties of SLs. The SLs of various types are considered, namely, strictly periodic, disordered, lattices with defects, etc. The structures intermediate between the periodic and disordered structures, or quasi-periodic lattices, e.g., the Fibonacci and the Thue–Morse SLs, occupy a special place among the SLs. This is associated with their unusual properties such as self-similarity, the Cantor nature of the energy spectrum, etc. (see, e.g., [2]).

However, starting from 2004, graphene-based structures attracted great attention, which is naturally explained by nontrivial properties of graphene, including electron ones. It is sufficient to call the analogy of π electrons of graphene with the Dirac massless fermions at low energies (which are formally described by the Dirac massless equation), the linear variance law, the chirality property, the Klein tunneling, the high mobility, the ballistic transport, the unusual Hall quantum effect, etc. [3–6]. It should be also taken into account that graphene is a promising material in modern electronics from the viewpoint of the substitution of the silicon technology, the development of which has come to its limit, by the graphene technology. It is evident that by virtue of the mentioned properties, the investigation of physical properties of graphene-based superlattices is an urgent problem [7–16]. Particularly, it is shown in [9, 10, 13] that a new Dirac point and the corresponding forbidden band manifest themselves in graphene SLs; it is determined through the zero value of the averaged wave number [9]. In new studies, the properties of this new gap in various graphene SLs are investigated in details. (For brevity, we will call this forbidden band as a "new Dirac" band, and we will call other gaps in the energy spectrum of the strictly periodic SL as well as the gaps in the Fibonacci SLs similar to them as the Bragg gaps [13, 14]).

A series of methods to form graphene SLs is suggested and implemented in practice [17–19]. We note that among other ones, it is important to obtain such graphene-based SLs, in which the forbidden band exists in the energy spectrum since just its presence plays the key role in the development of transistor-type semiconductor devices. Therefore, developers apply the efforts to the formation of graphene structures with the sufficiently wide gap. Here, using various methods such as the use of graphene nanoribbons, the interaction with the substrate, etc.; essential results are already attained [20–25]. Particularly, developers succeeded to obtain the gap several tenth of electron-volt wide by chemical methods [23].

2. CONCRETIZATION OF THE STATEMENT OF THE PROBLEM AND THE METHOD FOR CALCULATING THE SPECTRA

In this study, we investigate the energy spectrum of the graphene-based Fibonacci superlattices in a continual model. The quasi-periodic modulation along axis Ox is formed due to the mass summand in the Hamiltonian Δ: it accepts one of two different values in different elements in the SL chain according to the Fibonacci law. (Similar assumption for the formation of the SL was particularly considered in [16]). Mainly the SLs, in which the segments of zero-gap and nonzero-gap graphene are alternated by the Fibonacci quasi-periodic rule, are mainly investigated. By virtue of the essential progress in the technology of formation of the zero-gap graphene structures, we vary the values of Δ in rather broad limits; the nature of summand Δ in the Hamiltonian, as it was already mentioned, can be different.

Let us consider the SL constructed of two elements a and b presented in Fig. 1. Both elements contain a quantum well with width w and a potential barrier with width d; for element a, parameter Δ equals Δ_a, while the barrier height is denoted V_a; for element b, we have Δ_b and V_b, respectively. The SL is constructed according to the Fibonacci inflation rule: $S_n = S_{n-1} + S_{n-2}$. Therefore, for example, for the fourth Fibonacci generation (sequence), we have $S_4 = abaab$. Passage conditions of the electron wave through the SL constructed for the Nth Fibonacci generation are determined by the period of this generation. Energy ranges E, for which the transmission coefficient of electrons through the lattice $T(E)$ is close to unity, form the allowed bands in the energy spectrum, while forbidden bands correspond to energy segments with $T \ll 1$. Coefficient T can be calculated by the method of transfer matrices expressing it either through the Green's functions or through the wave functions. The latter can be found from the Dirac-type equation corresponding to the problem:

$$[v_F(\boldsymbol{\sigma}, \mathbf{p}) + m v_F^2 \sigma_z + V(x)\hat{\mathbf{I}}]\Psi = E\Psi, \qquad (1)$$

where $v_F \approx 10^6$ m/s is the Fermi velocity, $\mathbf{p} = (p_x, p_y)$ is the pulse operator, $\boldsymbol{\sigma} = (\sigma_x, \sigma_y)\sigma_x, \sigma_y, \sigma_z$ are the Pauli matrices for the pseudospin, $V(x)$ is the external potential, which depends on the coordinate x; $\hat{\mathbf{I}}$ is the unity two-dimensional matrix; we denote the mass summand by symbol Δ as it is accepted in publications. Function Ψ is a two-component pseudospinor $\Psi = [\tilde{\Psi}_A, \tilde{\Psi}_B]^T$, $\tilde{\Psi}_A$, $\tilde{\Psi}_B$ are the envelope functions for graphene sublattices A and B, and T is the transposition. Let us assume that potential $V(x)$ consists of periodically repeating rectangular barriers along axis Ox, and inside each jth barrier, $V_j(x) = \text{const}$. In this case, using the translational invariance of the solution over axis Oy, we can write $\tilde{\Psi}_{A,B} = \Psi_{A,B} e^{ik_y y}$, and we can derive for $\Psi_{A,B}$ from Eq. (1):

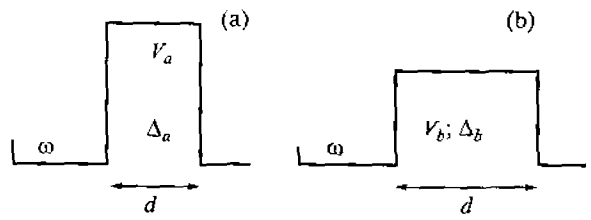

Fig. 1. Schematic representations of elements a and b constituting the superlattice.

$$\frac{d^2\Psi_{A,B}}{dx^2} + (k_j^2 - k_y^2)\Psi_{A,B} = 0, \qquad (2)$$

where $k_j = \text{sgn}(s_{j+})[(E - V_j)^2 - \Delta^2]^{1/2}$ $s_\pm \equiv E - V(x) \pm \Delta$, here and below, measurement units $c = \hbar = e = v_F = 1$. If we represent the solutions for eigenfunctions $\Psi_{A,B}$ is the form of the sum of planar waves moving in the direct and inverse directions along axis Ox, we derive

$$\Psi(x) = \left[a_j e^{iq_j x} \begin{pmatrix} 1 \\ g_j^+ \end{pmatrix} + b_j e^{-iq_j x} \begin{pmatrix} 1 \\ g_j^- \end{pmatrix} \right], \qquad (3)$$

where $q_j = \text{sgn}(s_{j+})\sqrt{k_j^2 - k_y^2}$, if $k_j^2 > k_y^2$, and $q_j = i\sqrt{k_y^2 - k_j^2}$ in the opposite case, $g_j^\pm = \dfrac{\pm q_j + ik_y}{k_y}$, the upper line in (3) is referred to sublattice A, and the lower one is referred to B. The transfer matrix, which associates wave functions in points x and $x + \Delta x$ is found in some studies (see, e.g., [9]), and has the form

$$M_j = \frac{1}{\cos\theta_j} \begin{pmatrix} \cos(q_j\Delta x - \theta_j) & iz_j^{-1}(q_j\Delta x) \\ iz_j \sin(q_j\Delta x) & \cos(q_j\Delta x + \theta_j) \end{pmatrix}, \qquad (4)$$

where

$$z_j = \frac{s_{j-}}{k_j}, \quad \theta_j = \arcsin\left(\frac{k_y}{k_j}\right).$$

The transmission coefficient of electrons through the lattice: $T = |t|^2$,

$$t = \frac{2\cos\theta_0}{R_{22}e^{-i\theta_0} + R_{11}e^{i\theta_0} - R_{12} - R_{21}}, \qquad (5)$$

where θ_0 is the incidence angle of the wave, while matrix R is expressed through the product of matrices M_j: $R = \prod_{j=1}^{N} M_j$, N is the total number of elements in the sublattice.

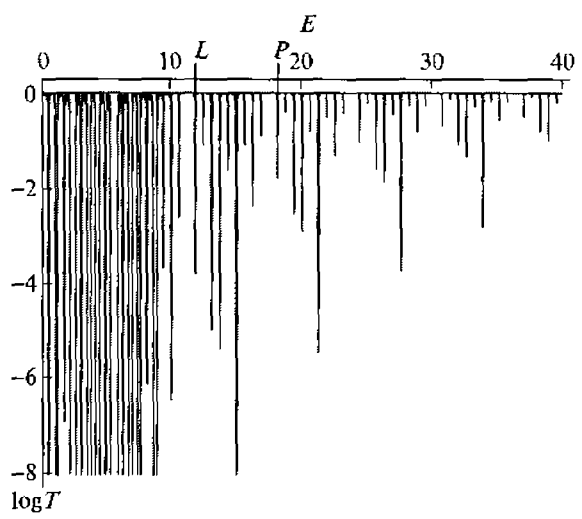

Fig. 2. Dependence of transmission coefficient T on electron energy E for the fourth Fibonacci generation. Values of parameters: $k_y = 0$, $d = w = 0.5$, $V_a = V_b = 5$, $\Delta_a = 1$, and $\Delta_b = 0$.

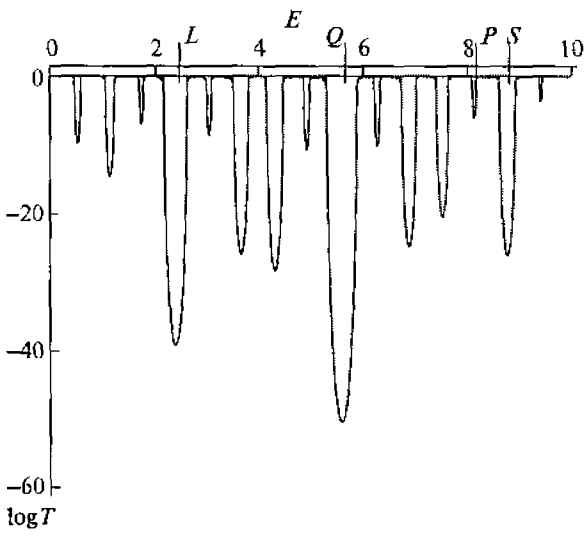

Fig. 3. Tunnel spectrum of the fourth Fibonacci generation in the energy range of [0, 10]. Parameters are the same as in Fig. 1.

3. RESULTS AND DISCUSSION

Figure 2 shows a part of the tunnel spectrum, i.e., the energy dependence of electron transmission coefficient T for the SL of the fourth Fibonacci generation under the condition of the normal incidence of the electron wave on the lattice ($k_y = 0$). Parameters of the problem are presented in Fig. 2; Fig. 3 represents the same spectrum in the energy range of [0, 10] (in addition, $V_a = V_b = 4$).

First of all, when analyzing the spectra, we should pay attention to the fact that the quasi-periodic modulation due to parameter Δ, which is used in this study, lead to very effective splitting the energy bands and thereby to the formation of a series of gaps. We emphasize that this is implemented with the normal incidence of electrons on the lattice.

Separate fragments can be distinguished in the spectra, the structure of which is periodically repeated over the entire energy scale; we can conventionally assume that one of these fragments of the spectrum is its period (for example, in the energy range LP in Fig. 2; in principle, we can also consider the narrower ranges: it is seen in Fig. 3 that the structure of fragments LQ and QS is similar). The characteristic features of the period is the number of the allowed (forbidden) bands; their widths vary upon going to higher E so that the width of gaps decreases as E increases on average; the natural result of this decrease is the fact that transmission coefficient T asymptotically approaches unity in a rather far overbarrier region.[1] The analysis of the spectra at high energies is out of the frameworks of our work, and we will further limit ourselves by energies of the order of several units in the accepted system of measurement units.

We here want to pay attention to a definite distinction of the situation from the situation in usual SLs (with the parabolic variance law of charge carriers). In contrast to usual SLs, where the bands are usually calculated over the entire barrier region [26, 27], it is appropriate to select definite energy ranges, for example, LQ, LP (see Figs. 1, 2, and footnote), or other fixed spectral ranges as applied to graphene structures.

The spectra similar to that presented in Fig.1 for the fourth generation are also implemented for other sequences.

The number of bands in each period and the width of each of them substantially depend both on the SL parameters on the one hand and on the number of the Fibonacci generation on the other hand.

Energy range LQ requires the special attention. The number of band in this energy range follows the inflation Fibonacci number: $Z_n = Z_{n-1} + Z_{n-2}$. This is confirmed in Fig. 4, where the bands of allowed energies (solid lines) and forbidden energies (intervals between the transmission bands, i.e., the gaps) are depicted. We note that this regularity is referred not only to the LQ range but also to large energy ranges,

[1] The variation in the band widths has the oscillating character rather than the monotonic one, and broadening and narrowing the band gaps is alternated as E increases. As a result, broader periods are formed (conventionally superperiods). In other words, the result of this wave-like variation in the band width is grouping of smaller separate structural units into larger ones with the formation of the additional structural order, and the self-similarity property manifests itself in this fact in our problem.

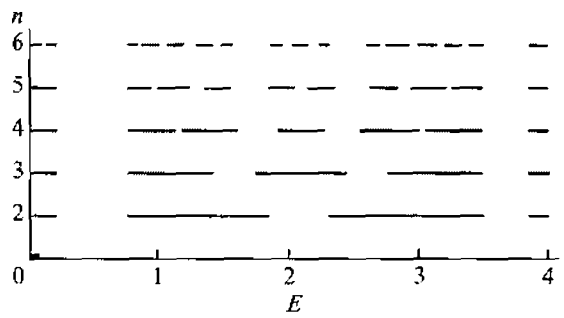

Fig. 4. Trace-map for the Fibonacci SL with parameters $k_y = 0$, $d = w = 0.5$, $V_a = V_b = 1$, $\Delta_a = 1$, and $\Delta_b = 0$.

namely, LP etc.; of course, each new superperiod has its own number of the bands.

It should be also noted that the formation of L and Q bands is associated with the periodicity factor, while the formation of the bands intermediate between them is associated with the quasi-periodicity factor. We can be easily convinced in this fact by means of calculating the spectrum for the strictly periodic lattice; for the same parameters, it has bands L and Q, which are arranged in the same points on the energy axis.

We can see in Fig. 4 that the forbidden band associated with new Dirac point E_D, or the "new Dirac gap" [9], is formed in all Fibonacci generations at definite energies. It location is almost invariable in various Fibonacci sequences. A characteristic feature of a new Dirac gap is the fact that it is independent of the lattice period $(d + w)$; however, it is very sensitive to the d/w ratio. This is also indicated by Figs. 5 and 6, where the $T(E)$ dependence for the fourth Fibonacci generation for various parameters d and w is shown. Let us ones more pay attention to the fact that the bands split (thereby with the formation of the series of the gaps) already in the case of the normal electron incidence on the SL surface. This result substantially differs from that found in [13], where the quasi-periodic modulation was formed due to the distinction in potentials of elements (a) barrier and (b) well, and manifested itself only for the inclined wave incidence ($k_y \neq 0$).

Figure 7 represents the set of allowed and forbidden bands for the fourth Fibonacci generation at various values of parameter Δ_a. It is seen that the effective band splitting is implemented in a broad range of Δ_a.

In the general case, the magnitude of E_D depends on each of parameters d, w, V_a, V_b, Δ_a, and Δ_b. It turns out that the Δ_a, Δ_b-dependence of E_D is not significant. For example, in the case $d = w$ and $V_a = V_b = V$, the location of a new Dirac point is mainly determined by the potential barrier height and only slightly deviates from $V/2$ as Δ_a increases (see all figures, $E_D = V/2$ is the exact location of a new Dirac point in the strictly periodic lattice [9]).

It is of interest to follow the variations in the band pattern depending on the ratio between quantities Δ_a and Δ_b since this is precisely the ratio that determines the efficiency of the quasi-periodic modulation in this study. This is done with the help of Fig. 8, in which the spectra of the fourth Fibonacci generation are shown for three values of ratio Δ_a/Δ_b, namely, at fixed $\Delta_a = 1$; the dashed, the dash-and-dot, and the solid lines correspond to values of $\Delta_b = 0.1$, 0.5, and 0.9. Other parameters are taken such as in Fig. 4. As the difference between Δ_a and Δ_b decreases, narrowing the gaps appeared under the effect of the quasi-periodic poten-

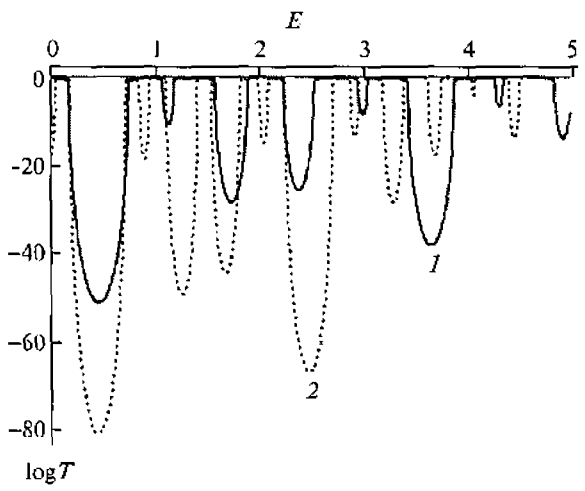

Fig. 5. Spectrum of the fourth Fibonacci generation for various lattice periods: (*1*) $d = w = 0.5$, (*2*) $d = w = 0.8$, other parameters as in Fig. 1.

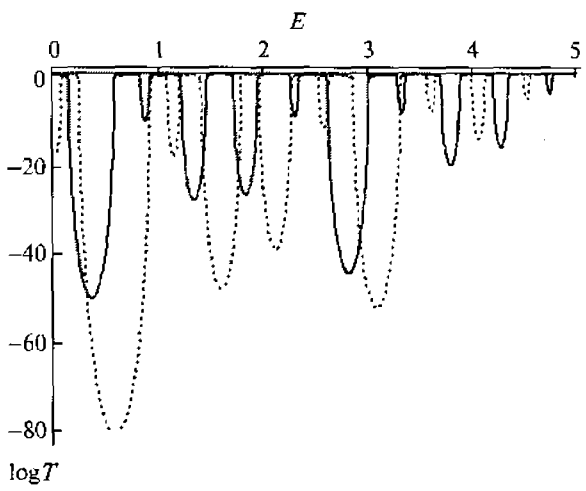

Fig. 6. Spectrum of the fourth Fibonacci generation for various d and w. The solid line corresponds to $d = 0.8$ and $w = 0.5$, the dashed line corresponds to $d = 0.5$ and $w = 0.8$, other parameters as in Fig. 1.

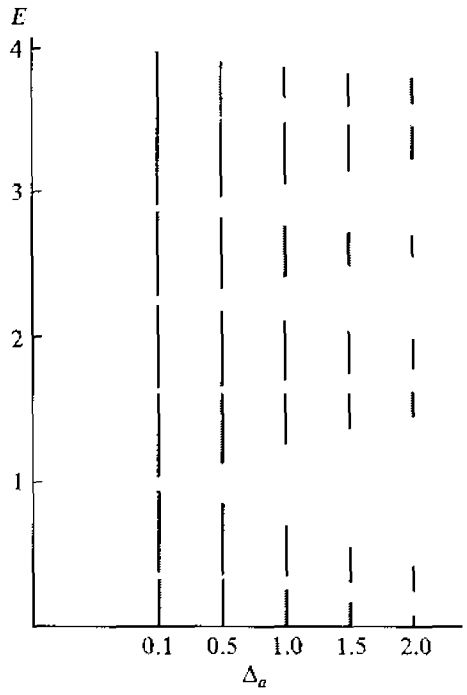

Fig. 7. Dependence of the spectrum of the fourth Fibonacci generation on parameter Δ_a; other parameters as in Fig. 1, $V_a = V_b = 2$.

tial up to their complete disappearance at $\Delta_a = \Delta_b$, i.e., in the case of the strictly periodic SL, is shown.

Figure 9 shows the band structure of the fourth Fibonacci generation in coordinates E, k_y, which shows the dependence of the spectra on the incidence angle of the wave. We note that a definite expansion of the Dirac gap is observed while the k_y-dependence of other forbidden bands is very weak. (It is known that a similar circumstance is often met when considered certain effects in graphene structures; particularly, a similar result is found in [11]: if the sufficiency strong effect is observed at $k_y = 0$, then its dependence on k_y is weak; see also the corresponding comment in this study). The dashed line in Fig. 8 corresponds to $E_D \approx V/2 = 0.5$ almost completely.

Figure 10 represents the results of the calculation of the conductance for the fourth generation of the SL under consideration by the known formula

$$G = G_0 \int_0^{\pi/2} T\cos\theta d\theta, \qquad (6)$$

where

$$G_0 = \frac{2e^2 m v_F L}{\hbar^2},$$

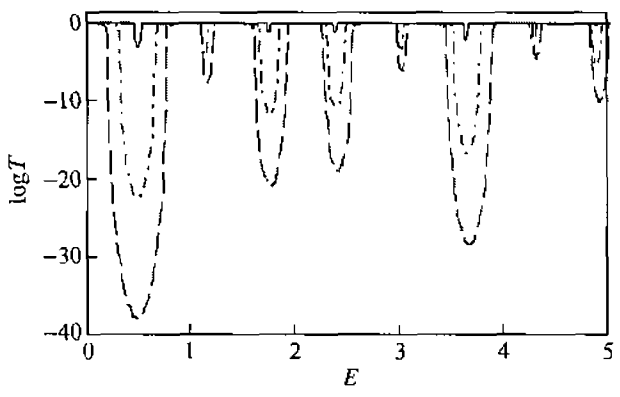

Fig. 8. Dependence of the spectrum of the fourth Fibonacci generation on the ratio between parameters Δ_a and Δ_b.

L is the width of the graphene sample along axis Oy, e is the elementary charge, m is the electron mass, and v_F is the Fermi velocity. The parameters are as follows: $k_y = 0$, $V_a = V_b = 2$, $\Delta_a = 1$, and $\Delta_b = 0$; for Fig. 10 (*1*), $d = w = 0.5$; and for Fig. 10 (*2*), $d = w = 0.8$. It is seen that the first conductance minimum is formed for the energy corresponding to the gap associated with a new Dirac point. As the lattice period changes, the location of this minimum remains invariable, while other minima are shifted along the energy axis. Thus, varying particularly lattice parameters d and w, we can control the conductance of the system under consideration.

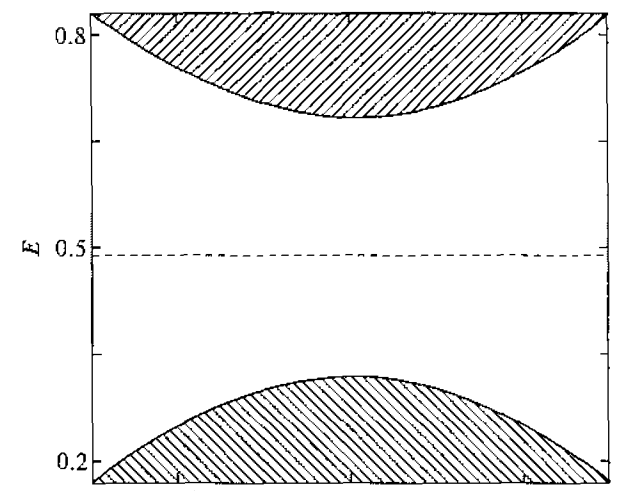

Fig. 9. Band structure of the spectrum of the fourth Fibonacci generation depending on parameter k_y. Parameters are the same as in Fig. 2.

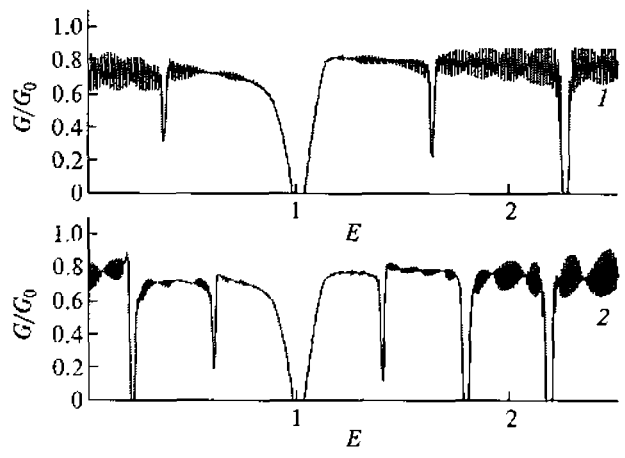

Fig. 10. Dependence of conductance of the SL of the fourth Fibonacci generation on energy E.

REFERENCES

1. R. Tsu, *Superlattice to Nanoelectronics*, 2nd ed. (Elsevier, Oxford, 2011).
2. Z. Cheng, R. Savit, and R. Merlin, Phys. Rev. B: Condens. Matter **37**, 4375 (1988).
3. A. K. Geim and K. S. Novoselov, Nat. Mater. **6**, 183 (2007).
4. A. N. Castro Neto, F. Guinea, N. M. R. Peres, K. S. Novoselov, and A. K. Geim, Rev. Mod. Phys. **81**, 109 (2009).
5. J. M. Pereira, F. M. Peeters, A. Chaves, M. Barbier, and P. Vasilopoulos, Semicond. Sci. Technol. **25**, 033002 (2010).
6. V. V. Cheianov and V. I. Falko, Phys. Rev. B: Condens. Matter **74**, 041403 (2006).
7. Q. Zhao, J. Gong, and C. A. Muller, Phys. Rev. B: Condens. Matter **85**, 104201 (2012).
8. M. Barbier, P. Vasilopoulos, and F. M. Peeters, arXiv:cond-mat/1101.4117 V1 (2011).
9. L. Wang and X. Chen, arXiv:cond-mat.mes-hall/1008.0504 V1 (2010).
10. L. Wang and S. Zhu, Phys. Rev. B: Condens. Matter **81**, 205444 (2010).
11. V. H. Nguyen, A. Bournel, and P. Dollfus, Semicond. Sci. Technol. **26**, 125012 (2011).
12. M. Barbier, P. Vasilopoulos, and F. M. Peeters, Phys. Rev. B: Condens. Matter **80**, 205415 (2009).
13. P. Zhao and X. Chen, arXiv:cond-mat.mes-hall/1111.1754 V1 (2011).
14. T. Ma, C. Liang, L. Wang, and X. Chen, arXiv:cond-mat.1754 V1 (2012).
15. Yu. P. Bliokh, V. Freilikher, S. Savel'ev, and F. Nori, Phys. Rev. B: Condens. Matter **79**, 075123 (2009).
16. P. V. Ratnikov, JETP Lett. **90** (6), 469 (2009).
17. J. C. Meyer, C. O. Girit, M. F. Crommie, and A. Zetti, Appl. Phys. Lett. **92**, 123110 (2008).
18. P. W. Sutter, J. Flege, and E. A. Sutter, Nat. Mater. **7**, 406 (2008).
19. J. Coraux, A. T. N'Diaye, C. Busse, and T. Micheli, Nano Lett. **8**, 565 (2008).
20. Y. W. Son, M. L. Cohen, and S. G. Louie, Phys. Rev. Lett. **97**, 216803 (2006).
21. M. Y. Han, B. Ozyilmaz, Y. Zhang, and F. Kim, Phys. Rev. Lett. **98**, 206805 (2007).
22. G. Giovanetti, P. A. Khomyakov, G. Brocks, P. Kelly, and J. van der Brink, Phys. Rev. B: Condens. Matter **76**, 073103 (2007).
23. S. Y. Zhou, G. Gweon, A. V. Fedorov, F. Guinea, A. H. Castro Neto, A. Lanzara, P. First, W. de Heer, and D.-H. Lee, Nat. Mater. **6**, 770 (2007).
24. R. Balog, B. Jorgensen, L. Nilsson, M. Anderson, E. Rienks, and M. Bianchi, Nat. Mater. **9**, 315 (2010).
25. S. Casolo, R. Martinazzo, and G. F. Tantardini, J. Phys. Chem. C **115** (8), 3250 (2011).
26. A. N. Korol', Phys. Solid State **36** (8), 1272 (1994).
27. A. N. Korol', JETP Lett. **59** (10), 695 (1994).

Translated by N. Korovin

SPELL: OK